

Contrast in Manganese Nodule Distribution on Either Side of 79° E Fracture Zone in Central Indian Basin

V. N. KODAGALI

National Institute of Oceanography
Dona Paula, Goa, India

Seabed topography is one of the prime factors in controlling the distribution of manganese nodules. Study of the nodule abundance on either side of the 79° E fracture zone in the Central Indian Basin (identified from multibeam bathymetric data) shows that the western side of the fracture zone has higher average nodule abundances. The eastern (downthrown) side of the fracture zone has less nodule abundance, and the seafloor is very smooth with a thick sediment layer. The sedimentation rates on the downthrown side are higher because of the sediment input from the northeastern direction and the fracture zone wall acting as a conduit for sediment transport. Immediately after the fracture zone on the eastern side, the seafloor is flat because of the sediment being deposited on the foot of the fracture zone. Also, the western flank seafloor has higher relief than the eastern flank. However, the metal content in nodules on either side does not show marked variations.

Keywords Central Indian Basin; fracture zone, manganese nodule abundance, multibeam data, sedimentation, topography

The economic potential of manganese nodules has led to increased efforts to understand the factors controlling their distribution. Important factors controlling the distribution of deep sea manganese nodules are: (1) low sedimentation rate (Glasby, 1973), (2) availability of nucleating material (Glasby, 1973; Horn et al., 1973), and (3) topography (Glasby, 1976; Craig, 1979; Usui et al., 1987; Kodagali, 1988; Pattan and Kodagali, 1988; Kodagali and Sudhakar, 1993).

Nodule distribution is related to conditions derived from plate tectonic factors, namely, the proximity to volcanic centers (availability of nucleating material), depth of seafloor, and topography (abyssal hill, fracture zone, and volcanic features).

Maximum nodule coverage occurs on steep slopes and local topographic highs such as hilltops, slopes, etc. (Frazer and Fisk, 1981) and in areas around the fracture zones (Clarion-Clipperton zone; Craig, 1979). In the Indian Ocean, nodule

Received 3 February 1994; accepted 23 March 1994.

The author is grateful to Mr. R. R. Nair, project leader and head, Geological Oceanography Division, for the encouragement and critical review of this manuscript. The director of the National Institute of Oceanography is thanked for facilities extended and for permission to publish this work. The Hydrosweep group is acknowledged for their help in data collection. Dr. V. K. Banakar is thanked for the helpful discussions.

Address correspondence to Dr. V. N. Kodagali, Geological Oceanography Division, National Institute of Oceanography, Dona Paula, Goa 403 004, India.

abundance was reported to be higher on high relief terrains (Pattan and Kodagali, 1988; Kodagali 1988, 1992; Kodagali and Sudhakar, 1993).

Multibeam swath bathymetric surveys have identified the southern extension of the 79° E fracture zone in the Central Indian Basin (Kamesh Raju et al., 1993; Kodagali, 1992). In order to understand the distribution of nodules around the fracture zone, nodule abundances were compared with fracture zone topography. The results are presented here.

Methods

Nodule sampling was carried out in the area (12°S to 14°30' S and longitudes 78°30' E to 79°17' E) using the free fall grabs (FFG) on four research ships (*ORV Sagarkanya*, *MV Skandi Surveyor*, *MV Farnella*, and *DSV Nand Rachit*). Figure 1 shows the trend of the fracture zone and the nodule sampling locations. A total of

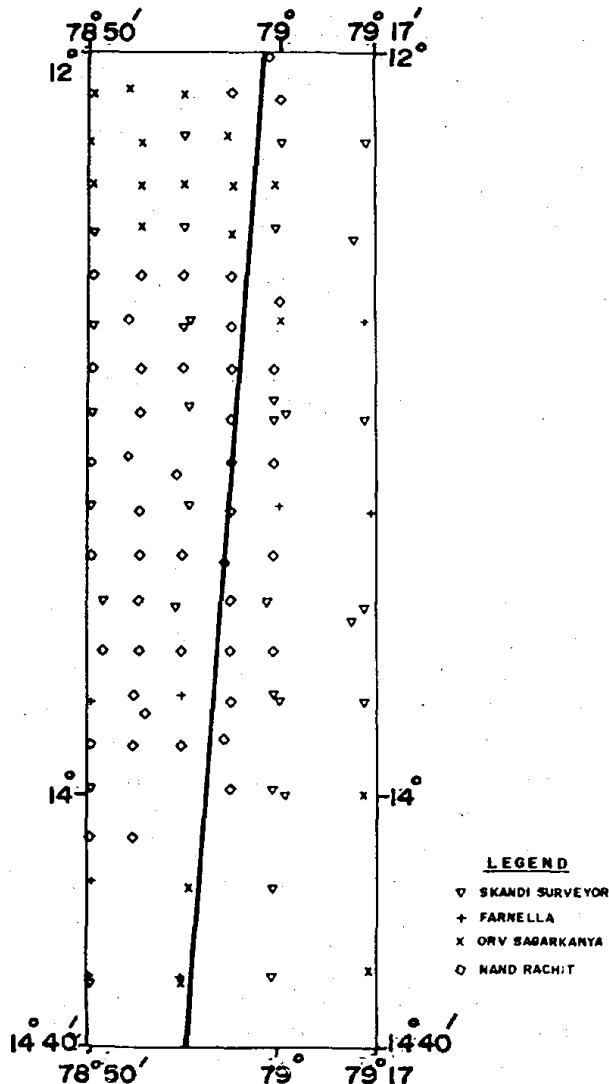


Figure 1. Sampling locations on either side of 79°E FZ are shown. Thick black line represents the trend of the fracture zone.

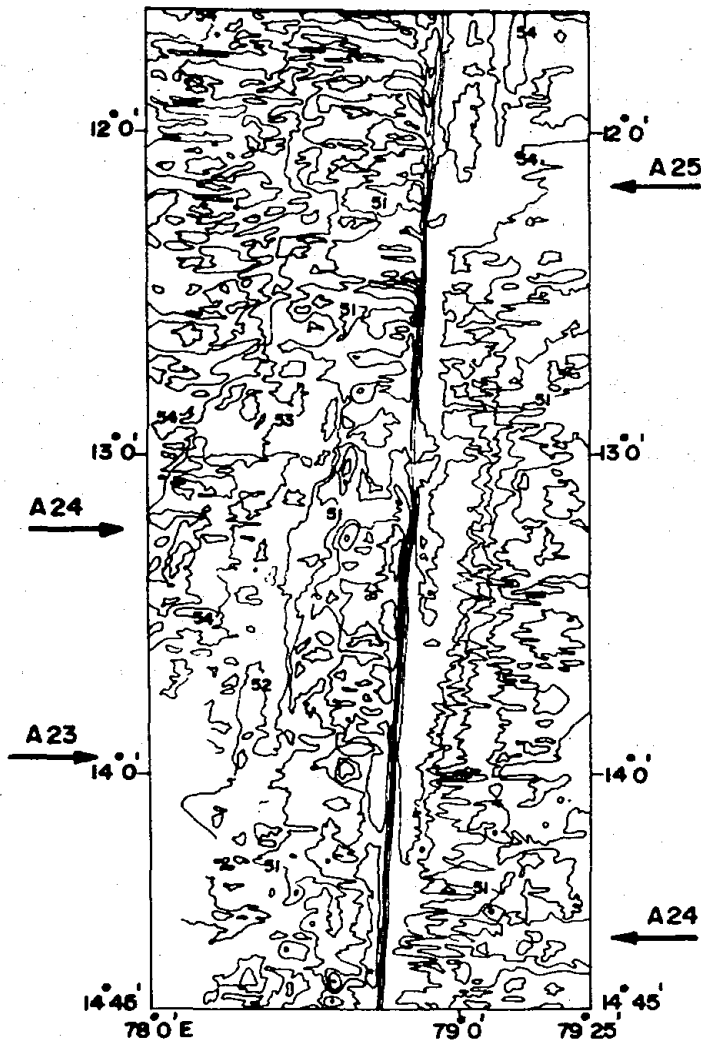


Figure 2. Regional bathymetric map (contour interval 100 m) of the study area with magnetic anomaly numbers.

67 stations were occupied on the west of the fracture zone, while 42 stations were on the east. At each sampling location, four to seven FFG were launched. By using the data from four to seven FFG at each station, the mechanical and other defects of sampling were minimized. The average abundance for the station was calculated by averaging the nodule abundances from all the grabs launched at the station.

The depth data was collected by Hydrosweep, the multibeam swath bathymetric survey system (for technical details see Gutberlet and Schenke, 1989) on board *ORV Sagarkanya* during October 1990. The survey was conducted along 16 north-south lines with a line spacing of five nautical miles. Hydrosweep operates at a frequency of 15.5 KHz, makes use of 59 preformed beams, and gives a swath coverage equal to twice the water depth. In the study area where the average depth was around 5100 m, the line spacing of 5 nm ensured complete coverage with slight overlap (Kamesh Raju et al., 1993). The Magnavox global positioning system (GPS) used in conjunction with the integrated navigation system (INS) on board the *ORV Sagarkanya* provided fairly accurate position data. Figure 2 gives the 100 m interval depth contour map of the study area clearly showing the fracture zone. Though the

fracture zone extension was identified from 10° 15' S to 14° 45' S, only a part of it (from 12° S to 14° 45' S) is reproduced in Figure 2 as the sampling locations are concentrated in this area.

Results and Discussion

Fracture Zone Topography

Figure 2 shows the regional bathymetric map constructed from the multibeam data. The contour interval is 100 m. Generally, the depth in this area varies between 5050 and 5400 m. The fracture zone topography is clearly depicted by the linear north-south trending contour lines (Kamesh Raju et al., 1993). Depth on the west of the fracture zone is around 5000 m and increases to 5400 m, with a high gradient on the east of the fracture zone (downthrown side). East-west cross-section profiles in Figure 3 (drawn from the gridded depth values) clearly show the fracture zone downthrow. The fracture zone shows a ridge-trough topography with overall relief of 300 to 500 m, which is similar to the Pacific fracture zones (Sandwell and Schubert, 1982). Also, the western flank has higher relief compared to the eastern flank. From Figure 2, it is observed that the seafloor is flatter at the immediate foot of the fracture zone scarp, which is approximately 10 to 20 km wide. With a characteristic smooth zone, the trough (eastern side) widens toward the north, resembling the Clipperton fracture zone topography. However, the Clipperton transform has lesser trough because of the sediments trapped in the trough (Wessel and Haxby, 1990). Gradient of the FZ is steeper in the south, while it is more gentle on the north (Kamesh Raju et al., 1993). Figure 4 schematically shows the FZ and the direction of sediment input.

Prominent east-west lineations extending up to 20 to 30 km in length with relief of 200 to 300 m shows the ridge parallel topographic fabric of the South East Indian Ridge (SEIR) during Eocene-Paleocene times. Bathymetric character of lineations at 13° to 14° S on the east of the fracture zone shows correlation with that between 11° and 12° S latitude on the west of the FZ, indicating a right lateral offset of oceanic crust across 79° E FZ (Kamesh Raju et al., 1993). This right lateral offset is also manifested by contrasting magnetic anomaly numbers on either side of the FZ. As seen in Figure 2, magnetic anomaly A-24 corresponds to 13° 10' S on the west of the fracture zone, while on the east it corresponds to 14° 35' S latitude.

The area south of 14° S latitude has numerous seamounts that have depth up to 1400 m. In contrast, the area north of 14° S has fewer seamounts on the west of the fracture zone and no seamounts on the east. Seamounts on the east of the fracture zone between 14° and 14° 15' S latitude are irregular shaped; some are double peaked and steep, while seamounts on the west are more regular.

Nodule Abundance

Details of nodule abundance on the east and western side of the fracture zone are tabulated in Table 1. There is a striking difference in nodule abundance on the two sides. Mean abundance on the east is 3.56 kg/m² and to the west it is 5.45 kg/m², though the minimum and maximum abundance observed are the same. The standard deviations also are comparable (4.29 and 4.76). The frequency distribution

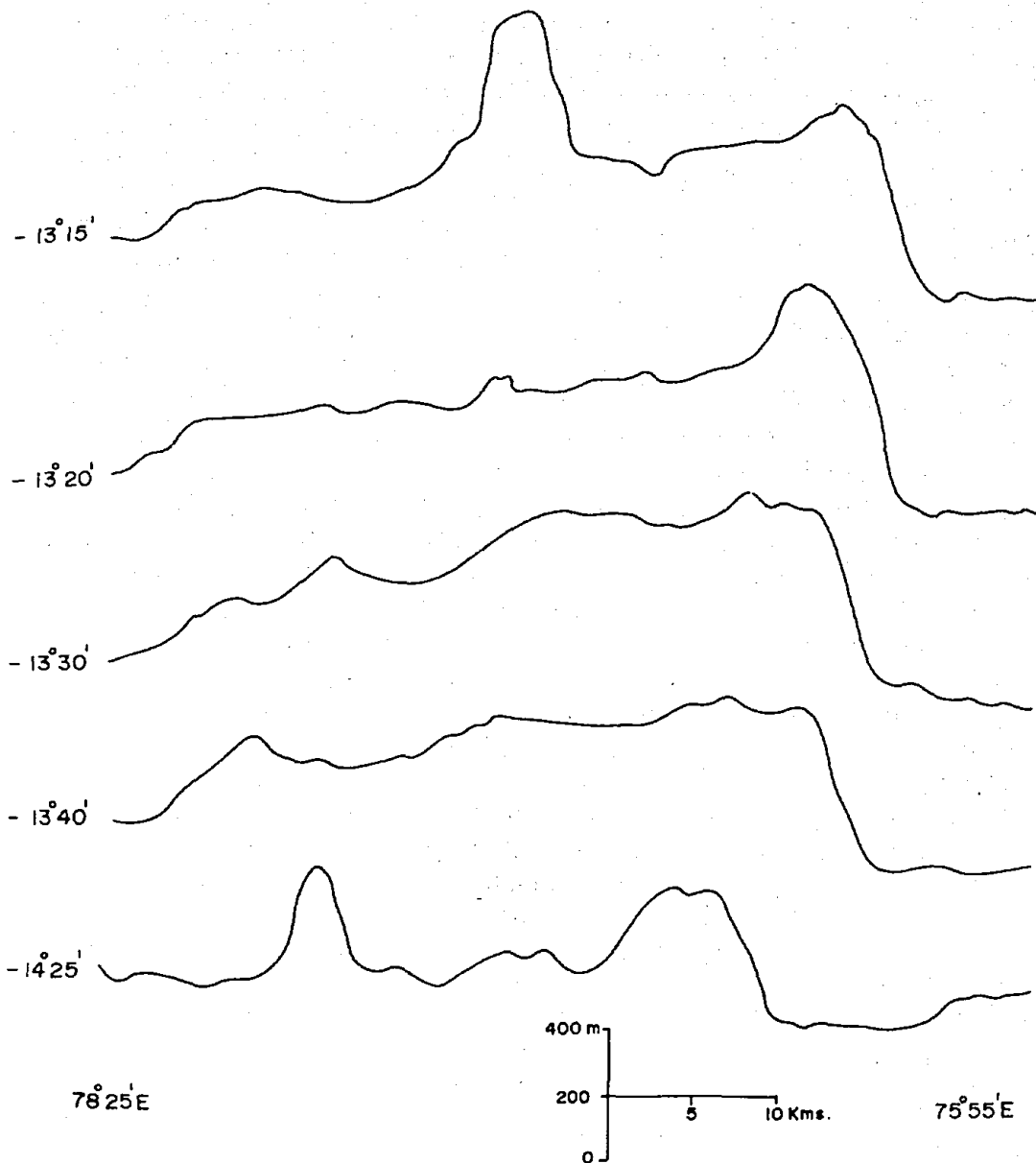


Figure 3. Cross-section profiles clearly showing the ridge crest topography across the fracture zones.

of nodule abundance (Table 2) shows occurrence of nil abundance for maximum cases on both the sides (17 out of 67 cases on the west and 15 out of 42 cases on the east). Although the distribution is Gaussian on both sides, the frequency distribution is perfectly skewed negatively on the east of the fracture zone. West of the fracture zone, an abundance value of 2 kg/m² appears 7 times, 5 kg/m² appears 8 times, and 8 kg/m² appears 6 times. East of the fracture zone, about 57% of cases have an abundance in the range 0 to 1 kg/m², bringing down the average for the area to 3.56 kg/m² only.

Fracture zones are linear features that originate as transform faults offsetting ridge crest. The fracture zones are reported to have a higher abundance of

Table 1
Details of nodule abundance on two sides of the fracture zone

Location	No. of stations	Nodule abundance				Biased variance
		Maximum (kg/m ²)	Minimum (kg/m ²)	Mean	SD	
East of fracture zone	42	17.5	0	3.56	4.29	17.95
West of fracture zone	67	17.5	0	5.45	4.76	22.34

nodules, the most well known being the Clarion-Clipperton fracture zone belt in the Pacific Ocean (Craig, 1979), which is considered to be the most promising for economic exploitation of the nodule deposits in the world. The nodule growth rates are higher especially near volcanic islands, seamounts, and fracture zones as they provide "seeds" for the nodules (Horn et al., 1973). Nodules from the vicinity of the Mendocino fracture zone have a growth rate of 40 to 81 mm/10⁶ years (Andrews, 1976). It is therefore assumed that volcanic influences and fracture zone

Table 2
Frequency distribution of nodule abundances on two sides of the fracture zone

Abundance value range (kg/m ²)	East of fracture zone		West of fracture zone	
	Frequency	Percent	Frequency	Percent
0	15	35.7	17	25.4
0.1-1	9	21.4	5	7.5
1-2	2	4.8	7	10.4
2-3	2	4.8	2	3.0
3-4	2	4.8	2	3.0
4-5	3	7.1	8	11.0
5-6	2	4.8	2	3.0
6-7	1	2.4	3	4.5
7-8	0	0	6	9.0
8-9	0	0	4	6.0
9-10	3	7.1	1	1.5
10-11	0	0	3	4.5
11-12	1	2.4	2	3.0
12-13	1	2.4	0	0.0
13-14	0	0	2	3.0
14-16	0	0	2	3.0
16-17	1	2.4	1	1.5
Total	42	100.0	67	100.0

may enhance growth of nodules, especially having higher growth rates intermittently and instantly bringing the average higher (Andrews, 1976).

Fracture zone regions show rugged topography and marked changes in depth of seafloor across the zone. It is observed in the present case that the depth difference across the zone is up to 400 m. The eastern side, the downthrown side, is rather flat near the fracture zone scarp. In general, the western side is more rugged. The east-west lineations of 100 to 150 m highs and lows are distinct and predominant in the western flank (Kamesh Raju et al., 1993) and thus render this side rougher. Though there are several seamounts and abyssal hills on the eastern flank, south of 14° S latitude, this flank is plain from 12° to 14° S.

The higher nodule abundance on the western side of the fracture zone may be because of the higher ruggedness of the seafloor there. Formation of nodules depends on availability of substrata (nucleus) in an oxidized environment (Horn et al., 1973). Abyssal sedimentation also influences nodule development. Rapid sedimentation hinders nodule growth by burying nodules and potential nuclei (Kodagali, 1988). Sediment movement from hills to flat areas decreases nodule development. Hence, regions of rugged relief (with low sedimentation rate and low sediment thickness) are likely to have a higher abundance of nodules than the flat area (with thick sediments and higher sedimentation rate). Seamounts and abyssal hills on the western side of the fracture zone have distinctive high relief and appear to have had periods of volcanic activity even after the generation of the seafloor in the region. These areas present a unique environment for nodule development due to the depth variations, availability of volcanic materials, and so forth.

In contrast, the eastern side of fracture zone is bordered by a comparatively flat region having a seafloor that is less rugged. The flatness of the seafloor is conspicuous in the 10- to 20-km belt next to the downthrow on the eastern flank. The reason for the eastern region being plain can be attributed to high sedimentation rates. At deep sea drilling project (DSDP) site 215, which is also on the eastern side of the 79° E fracture zone, the sedimentation rates are high. Bengal fan, which is almost 1000 km wide and 3000 km long, has more than 12 km of sediment thickness (Curry and Moore, 1971). Turbidity currents transport the sediments from the Ganges and the Brahmaputra river delta through the Swatch of No Ground into an extensive crisscrossing network of meandering valleys in Bengal fan and Nicobar fan. DSDP sites 215, 216, and 218 (all of which lie on the west of the 900 E ridge, nearer to the present study area) have an abundance of terrigenous sediments of Ganges-Brahmaputra source (Selater et al., 1974). Sites 218 and 211 penetrated thick sequences of terrigenous sediments belonging to the Bengal and Nicobar fans. The terrigenous sediments at site 215 were dated as from the late Miocene period (Pimm, 1974); this is the time when nodule growth in the Central Indian Basin was initiated. On the northwestern side of the present area, geochemical evidence for terrigenous input exists in the surface sediments (Nagendranath et al., 1989). It is, therefore, assumed that the terrigenous input from the northeastern side was prevalent in the study area (Figure 4). Also, the varying downthrow of the fracture zone and width of the flat area near the downthrow from north to south of the fracture zone suggest that the sediment input must have been directed from the north.

Fracture zone offsets do vary as a function of the age contrast across the fracture zone. However, in the case of the 79° E fracture zone, the lesser offset on the north is clearly because of the higher sediment input there (Kamesh Raju et

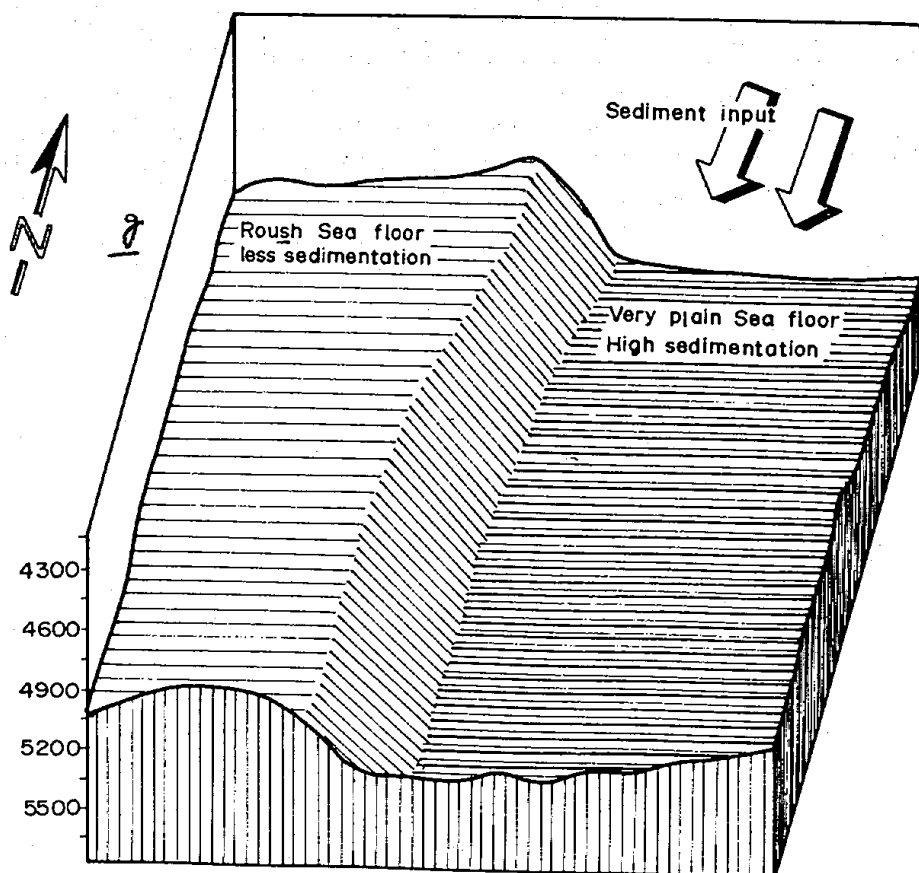


Figure 4. Schematic diagram of the fracture zone showing the sediment input from the NE direction.

al., 1993). The question arises then of why the sedimentation rates are high on the east, while just a few kilometers on the west of the fracture zone, they are less. Though the sediment thickness is known to vary over short distances (Johnson, 1972), it is influenced by the bathymetric relief. The valley at the foot of the fracture zone is acting as a conduit for sediments. It is possible that the bulk of the sediment input is under traction (because of bottom currents rather than by suspension). The downthrow as seen in cross-section profiles (Figure 3) is sharp and sudden and it may act as a barrier preventing the sediments from being deposited on the west of the fracture zone. Because of this barrier of fracture zone, the seafloor is flat on the east and there is a thick layer of sediments because of higher sedimentation rate, which also inhibits the nodule growth, resulting in less nodule abundance. Also, as seen in Figure 1, the sample locations on the western flank are scattered all over, while those on the eastern flank are concentrated near the downthrow, which incidentally is very plain. That is why in this case there is striking variation in nodule abundance a few kilometers apart. The study also confirms the earlier reports (Craig, 1979; Kodagali, 1988; Kodagali and Sudhakar, 1993) that the nodule abundance is higher on rough terrains and less on the flat regions.

Table 3
Chemical data for nodules from eastern side of fracture zone
(results from 24 stations)

Element	Minimum	Maximum	Mean	SD
Cu	0.38	1.72	0.940	0.390
Ni	0.58	1.51	1.010	0.263
Co	0.09	0.22	0.137	0.028
Ni + Co + Cu	1.08	3.18	2.097	0.631
Fe	4.03	13.00	7.898	2.468
Mn	17.40	30.33	24.648	3.363
Mn/Fe	1.45	7.78	3.453	1.339

Metal Content of Nodules

Results of bulk chemical analyses on nodules from both sides of the fracture zone are presented in Tables 3 and 4. The chemical data used here are from Banakar et al. (1989), and the analyses were carried out by standard atomic absorption spectrophotometer (AAS) techniques. Though there is a contrast in nodule abundances, the metal content does not have any surprises. Metal content of nodules on both sides of the fracture zones are similar. Mean nickel content, copper content, total metal content, and manganese content are higher on the eastern side of the fracture zone. The iron content, cobalt content, and Mn/Fe ratio are higher on the western side. However, the difference is marginal. Elsewhere in the world oceans it is observed that the cobalt content is higher around the fracture zones, more so on the downthrown side (Andrews, 1971). On this fracture zone, the cobalt content is high—up to 0.29%—but the mean cobalt content is higher on the western side (0.156). The mean cobalt content on the downthrown side is 0.138. The eastern side has lesser abundance and higher total metal content, indicating inverse relation between grade and abundance. The cobalt content is inversely related to total metal content; therefore, on the western side, cobalt is higher while the total metal content is less. It is concluded that the higher cobalt content is not related to the

Table 4
Chemical data for nodules from western side of fracture zone
(results from 38 stations)

Element	Minimum	Maximum	Mean	SD
Cu	0.28	1.52	0.897	0.366
Ni	0.39	1.55	0.942	0.276
Co	0.09	0.29	0.156	0.047
Ni + Co + Cu	0.90	3.18	2.002	0.600
Fe	4.18	16.96	8.039	2.896
Mn	15.64	33.51	24.201	3.997
Mn/Fe	1.02	7.49	3.515	1.508

downthrown side of the fracture zone but is related to iron content and the lesser total metal content (Ni + Cu + Co).

The interelement relations are also on the predicted lines on the two sides of the fracture zones. On the eastern side, Mn and Ni + Cu + Co are strongly correlated ($r = 0.64$), as are Mn and Ni ($r = 0.68$) and Mn and Cu ($r = 0.59$). On the western side, Co and Fe and Mn and total metal content are positively correlated ($r = 0.63$ and $r = 0.54$, respectively). Mn and Co are weakly inversely related on both sides ($r = -0.3$). Fe has a strong negative correlation with Cu, Ni, and Mn on the western side, while the negative correlations are weaker on the eastern side.

Summary

The presence of the 79° E fracture zone has strong influence on the distribution of nodules. The downthrown side (east) has less abundance. The ridge crest topography of the fracture zone has influenced the sedimentation pattern in the region, resulting in higher sedimentation on the eastern side, which probably originated from the Bengal fan and the Nicobar fan. The other reason for higher abundance on the western flank is the higher relief as compared to the eastern side. The metal contents do not show much variation. However, the cobalt content is more in the area west of the fracture zones, and it is marginally less on the downthrown side.

References

- Andrews, J. E. 1971. Abyssal hills as evidence of transcurrent faulting on north Pacific fracture zones. *Geological Society of America Bulletin* 82:463-470.
- Andrews, J. E. 1976. Aspects of geologic setting of manganese nodule deposits. In: Technical Bulletin No. 2. Paper presented at IDOE workshop, Sova, Fuji, September 1975. CCOP/SOPAC: 713-725.
- Banakar, V. K., J. N. Pattan, P. Jauhari, V. K. Padmavati, and G. Parthiban. 1989. Grade estimation of ferromanganese nodules collected during Nand Rachit cruises from Central Indian Basin. Internal report, PMN project NIO, Goa, India.
- Craig, J. D. 1979. Relationship between bathymetry and ferromanganese deposits in the north equatorial Pacific. *Marine Geology* 29:165-186.
- Curry, J. R. and D. C. Moore. 1971. Growth of the Bengal deep-sea fan and denudation of the Himalayas. *Geological Society of America Bulletin* 82:563-572.
- Frazer, J. and M. B. Fisk. 1981. Geological factors related to characteristics of sea floor manganese nodule deposits. *Deep Sea Research* 28(12):1533-1551.
- Glasby, G. P. 1973. Distribution of manganese nodules and lebensspuren in underwater photographs from Carlsberg ridge, Indian Ocean. *New Zealand Journal of Geology and Geophysics* 16:1-17.
- Glasby, G. P. 1976. *Marine manganese deposits*. Amsterdam: Elsevier.
- Gutberlet, M. and H. W. Schenke. 1989. Hydrosweep—New era in high precision bathymetric surveying in deep and shallow waters. *Marine Geology* 33(1):1-24.
- Horn, D. R., B. Horn, and M. N. Delach. 1973. Factors which control the distribution of ferromanganese nodules and proposed research vessel's track in North Pacific. Technical report of International Decade Ocean Exploration, 8-20.
- Johnson, D. A. 1972. Ocean floor erosion in the equatorial Pacific. *Geological Society of America Bulletin* 83:3121-3124.
- Kamesh Raju, K. A., T. Ramprasad, V. N. Kodagali, and R. R. Nair. 1993. Multibeam bathymetric, gravity and magnetic studies over 79° E fracture zone—Central Indian Basin. *Journal of Geophysical Research* 98B:9605-9618.

- Kodagali, V. N. 1988. Influence of regional and local topography on the distribution of polymetallic nodules in the Central Indian Ocean Basin. *Geo-Marine Letters* 8:173-178.
- Kodagali, V. N. 1992. Geomorphology of the Central Indian Basin and the influence of topography on the distribution of polymetallic nodules. Ph.D. thesis submitted to Goa University, India.
- Kodagali, V. N. and M. Sudhakar. 1993. Manganese nodule distribution in different topographic domains in Central Indian Basin. *Marine Georesources and Geotechnology* 11(4):293-308.
- Nagendranath, B., V. Purnachandra Rao, and K. P. Becker. 1989. Geochemical evidence of terrigenous influence in deep-sea sediments up to 80S° in the Central Indian Basin. *Marine Geology* 87:301-313.
- Pattan, J. N. and V. N. Kodagali. 1988. Seabed topography and distribution of manganese nodules in the Central Indian Ocean. *Mahasagar* 21(1):7-12.
- Pimm, A. C. 1974. Sedimentology and history of north east Indian Ocean from late cretaceous to recent. In: Initial reports DSDP National Science Foundation, Washington XXII, 717-803.
- Sandwell, D. T. and G. Schubert. 1982. Lithospheric flexure at fracture zones. *Journal of Geophysical Research* 87:4657-4667.
- Sclater, J. G. et al. 1974. Regional synthesis of the deep sea drilling results leg 22, East Indian Ocean. In Initial reports DSDP National Science Foundation, Washington, XXII, 815-831.
- Usui, A., A. Nishimura, M. Tanahashi, and S. Terashima. 1987. Local variability of manganese nodule facies on small abyssal hills of the Central Pacific Basin. *Marine Geology* 74:237-275.
- Wessel, P. and W. F. Haxby. 1990. Thermal stresses, differential subsidence, and flexure at oceanic fracture zones. *Journal of Geophysical Research* 95:375-391.